

Teaching polaritons new tricks

P G Savvidis^{1,2} and P G Lagoudakis¹

¹ Department of Physics and Astronomy, University of Southampton, SO17 1BJ, UK

² Physics Department, UCSB, Santa Barbara, CA 93106, USA

Received 11 March 2003, in final form 11 July 2003

Published 3 September 2003

Online at stacks.iop.org/SST/18/S311

Abstract

Semiconductor microcavities have attracted much recent interest because they utilize simultaneously 2D confinement of both excitons and photons in the same heterostructure. Strong coupling of these two states produces unique dynamics that can be well described in a quasiparticle state, the cavity polaritons. Their dispersion relation is dramatically modified with an apparent trap in k -space offering exciting new possibilities for tailoring nonlinear optical properties in microcavities. The reduced density of states inside the trap allows the macroscopic occupancy of polaritons producing much of the new physics. This paper describes recent work on nonlinear effects in semiconductor microcavities including stimulated scattering, parametric oscillation and non-equilibrium phase transition. By teaching polaritons new tricks, both fundamental questions about their bosonic nature can be answered and practical applications in a variety of optoelectronic and interferometric devices can be found.

1. Introduction

One of the major trends of modern semiconductor research is towards the achievement of electron and photon states of low dimensionality. Photons can be localized by periodic modulation of the refractive index of a medium, with a modulation length of the order of 100 nm or below, and comparable with the wavelength of light. By introducing a defect in a three-dimensional photonic crystal it is possible to achieve a full three-dimensional localization of light. On the other hand, charge carrier confinement has been widely exploited in quantum nanostructures such as 2D quantum wells, 1D quantum wires and 0D quantum dots. Control of the spontaneous emission rate by means of the photon density of states is of great practical importance as it can lead to novel light-emitting devices, including low threshold and inversionless lasers. Semiconductor microcavities offer opportunities for engineering such light–matter interactions by utilizing 2D photon and exciton confinement in the same heterostructure (figure 1(a)) [1, 2].

Polaritons result from strong coupling of high effective mass quantum well (QW) excitons and much lighter cavity photons (figure 1(b)). The resulting polariton dispersion is highly non-parabolic and its distinctive feature is the apparent dispersion around $k = 0$ which we call the polariton ‘trap’ (figure 1(c)). It is caused by the anticrossing of the exciton and photon branches when their energies are degenerate. The depth of the trap is determined by the strength of the exciton–

photon interaction and is typically of the order of few meV for III–IV semiconductors. Polariton energies inside the trap are substantially below all other states in the microcavity. Therefore, polaritons in the trap are well protected from phase scattering processes such as interactions with the phonons. Additionally, the relaxation bottleneck at the neck of the trap prevents other exciton–polaritons from scattering into the trap. More importantly the density of states inside the trap is dramatically reduced due to the very steep polariton dispersion. The resulting effective mass of polaritons is smaller by as much as 10^{-4} times the exciton mass. Correspondingly, the de Broglie wavelength for polaritons is thus also much longer. Since the achievement of quantum degeneracy requires the inter-particle separation to be comparable with the de Broglie wavelength, polaritons are very good candidates because this condition can be satisfied at very low carrier densities before any saturation occurs. The reduced density of states and light effective mass of polaritons with their dramatically modified dispersion relation opens new avenues for teaching polaritons new tricks. In this paper we demonstrate just how many interesting and rich phenomena arise as a result of scattering of polaritons on the lower polariton branch and the walls of the trap.

Polariton dynamics has been a subject of intensive investigation in the past few years. What makes polaritons especially interesting is that they possess integer spin and are expected to obey Bose–Einstein statistics at low densities [3, 4]. One of the distinct features of Bose particles is

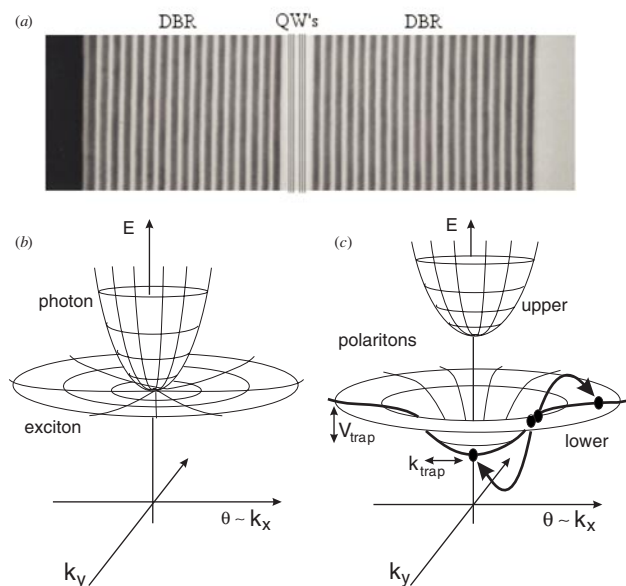


Figure 1. (a) Scanning electron microscopy (SEM) image of a semiconductor microcavity (SM). (b) Bare exciton and photon dispersions in SM. (c) In-plane 2D polariton dispersion relation, and formation of a polariton energy–momentum trap. Stimulated scattering mechanism is shown with arrows.

their final state stimulation. Indeed non-resonant excitation experiments have been used to successfully demonstrate polariton nonlinearities at the bottom of the trap [5–7]. A threshold in the luminescence from the lower polariton branch is observed and attributed to polariton stimulation due to the final state occupation. Although such behaviour was first proposed for excitons [8], their mass is $\sim 10^4$ times higher than the mass of polariton and hence the density of states is also much higher making the achievement of macroscopic occupancy almost impossible. At densities required for such macroscopic occupancy, excitons are ionized into an electron–hole plasma at which point they no longer exhibit bosonic properties.

Cavity polaritons are much easier to study than their 3D counterparts because in microcavities the critical wavevectors (wavevectors at which cavity dispersion and exciton dispersion intersect, strong coupling region) can be directly accessed by injecting photons at different angles. This contrasts with bulk polaritons where the light cone prohibits direct excitation of these states and the use of second-order processes is required [9, 10]. When a photon is absorbed in the microcavity structure, the in-plane component of the photon momentum is conserved, coupling directly to the polariton mode with the same in-plane momentum. This means that a specified polariton state can be pumped by choosing the angle of incidence of the laser beam that creates the polaritons. In the same way, the number of polaritons in a specific state can be detected by observing the photon emission only at a selected angle. Because the angle of incidence can be determined very accurately, these experiments therefore offer the possibility of studying the polariton momentum distribution near $k = 0$ with very high accuracy.

The paper is organized as follows. In section 2 stimulated polariton scattering under resonant excitation is

discussed. In the same regime, section 3 presents the asymmetric emission in k -space. The spin dynamics of the stimulated polariton scattering are analysed in section 4. Section 5 shows that a microcavity can operate as an optical parametric oscillator. Section 6 describes the conditions and the physical processes under which microcavities operate as ring emitters. Section 7 presents in a simplified manner the basic ideas of Bose–Einstein condensation phenomena in semiconductor microcavities followed by section 7 with concluding remarks and speculations for the future of strongly coupled microcavities.

2. Resonant stimulated scattering of polaritons

In this section we discuss the progress in understanding nonlinear optical properties of polaritons and their scattering dynamics by using experiments with resonant polariton injection and temporal and angular resolutions. By constructing a prototype pulsed-goniometer we directly probed the dispersion relation of these quasiparticles and examined their angular properties [11, 12]. Ultrafast laser pulses of approximately 100 fs duration allowed us to resolve carrier dynamics on sub-ps timescales.

In semiconductor microcavities crucial wavevectors can be accessed by directly injecting light at different angles and thus provide important information about the scattering dynamics and elucidate very rich angular properties of semiconductor microcavities. Such experiments are crucial in identifying the scattering processes on the polariton branch. The concept of a two-beam experiment is that the first pulse (pump) is used for excitation of the system, whereas the relaxation dynamics is probed by a weak (probe) pulse. In the experiments below, the pump beam is spectrally filtered to resonantly excite only the lower polariton branch. We demonstrated that if a pulse of polaritons is injected at the point of inflection on the side of the polariton trap $k = k_p$ (the so-called magic angle), they can pair scatter to yield a polariton at the bottom of the trap $k = 0$ (termed the signal) and a polariton that carries off the excess energy and momentum $k = k_{2p}$ (the idler) [11]. Such efficient polariton scattering is achieved when the final state at $k = 0$ is seeded by the probe beam. This process is depicted in figure 1(c) and it results in amplification of the incident probe beam by at least two orders of magnitude. Unambiguous proof for such scattering processes is provided by the observation of a third emitted beam corresponding to the idler wavevector. We show that the angle at which pump polaritons are injected is critical and its sharp angular resonance [11] is set by the energy and momentum conservation condition in the scattering process of two pump polaritons on the lower polariton branch. The magnitude of the amplification is dramatically suppressed when the energy and momentum conservation condition is not satisfied, explaining why this process has escaped observation for so long.

The ultrafast nature of the scattering process is revealed by temporally and spectrally resolved measurements. Figure 2 shows reflectivity spectra taken at normal incidence when the microcavity is pumped at the magic angle. The gain builds up on a scale of few ps and switches off as soon as the two pulses are not overlapping in time (figure 2). In contrast to

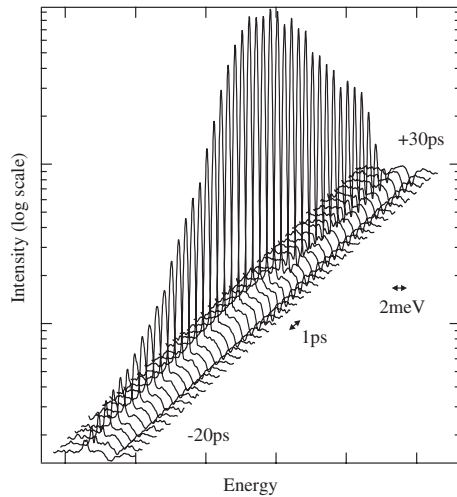


Figure 2. Probe beam reflectivity spectra taken at time delays between -20 ps and $+30$ ps. The gain builds up over few ps timescale and switches off when pump and probe beams no longer overlap in time. Microcavity recovers completely to its original state after ~ 30 ps.

other reports [13, 14], the excitation density is kept low so that polaritons survive and the exciton is unbleached. What is clear from our experiments is that this process relies on the bosonic property of polaritons to accumulate in a single quantum state via stimulated scattering. This is evidenced by the exponential power dependence of the gain on the pump power [11]. Indeed the *scattering rate* into the final state is enhanced by a factor of $1 + n_{\text{final}}$, where n_{final} is the number of polaritons in the final state and is linearly dependent on pump density according to $(1 + n_{\text{final}})n_{\text{pump}}$. The ultrafast nature of this stimulated scattering process and the fast recovery of the system to its original state after excitation due to the fast radiative lifetime of polaritons are now to be exploited for switching applications.

The observed polariton amplification has been successfully described within a model of interacting polaritons [15]. In the following we call this process ‘parametric’ in analogy with the well-known situation in nonlinear optics. According to this theory, polariton–polariton interactions are responsible for the parametric scattering. Polariton–polariton interactions are governed by Coulombic exciton–exciton interactions and exciton saturation. In the specific pump–probe configuration considered above, both pump and probe beams are coherently driving polarization at the corresponding wavevectors $k = k_p$ and $k = 0$ creating coherent and macroscopic populations at these wavevectors. Polariton populations also necessarily result from the amplitude of the polarization field. Polariton–polariton interactions efficiently couple polarizations at the signal, pump and idler wavevectors provided the energy and momentum conservation condition is satisfied (parametric coupling). Parametric coupling of polarizations at the signal, pump and idler wavevectors in the language of polariton populations means conversion of pump polaritons into the signal and idler modes. The generation rate for the probe polarization is proportional to its current magnitude meaning that the scattering or conversion rate is proportional to the final state occupation. Hence, the scattering of pump polaritons is stimulated by the probe pulse. It turns

out that because interactions between polaritons possessing the same spin are repulsive, the renormalized energy of the polariton branch is slightly blueshifted [15]. This blueshift is very apparent in the experimental data. An immediate result of this analysis is that the pump parametric conversion is not limited to the particular pump–probe configuration but should exist for any pair scattering in which energy and momentum are conserved. Experiments in section 3 demonstrate that indeed such pair scattering processes occur and in fact are dominating the mechanisms for relaxation of pump polaritons on the lower branch in the absence of the probe.

3. Asymmetric angular emission

In this section we show that light emission from microcavities in the parametric amplification regime is highly asymmetric due to the highly efficient relaxation of polaritons via pair scattering on the lower polariton branch and fast radiative emission before any thermalization takes place [12]. This is in strong contrast to light emission from other semiconductor heterostructures such as LEDs and VCSELs, where light is emitted symmetrically with respect to the sample normal. Angularly resolved luminescence experiments [12] allowed us to understand the processes that govern the relaxation of resonantly injected pump polaritons at a critical angle. Figure 3 shows the contour plot of PL spectra taken at angles ranging from -50° to $+50^\circ$ with and without the presence of the probe beam. It is important to note that the pair scattering process does not necessarily require the presence of the probe pulse but has a spontaneous component. In the absence of the probe beam the emission at many positive angles is dominated by the pair polariton–polariton scatterings which conserve energy and momentum. This is completely suppressed at negative angles. A simple model [12] which takes into account the radiative lifetime and exciton scattering rates reproduces exactly the observed intensities. Introduction of a weak probe pulse, figure 3(b), reorganizes dramatically the emission pattern. The injected probe pulse redistributes the light emitted at each angle and causes efficient probe-induced scattering into the bottom of the trap, extracting most of the available polaritons before other allowed pair scattering processes can act.

4. Spin dynamics of the stimulated scattering of polaritons

Hitherto, we have described the stimulated polariton scattering without any reference to spin. We have implicitly assumed that all polaritons have the same spin. In this section we give a short review of the spin dynamics of the resonant stimulated polariton scattering and describe a phenomenological approach to the problem. Polaritons see each other through their exciton fractions. Therefore, polariton spin dynamics originates from the spin of their exciton fraction. In what follows we will restrict ourselves to polaritons formed from heavy hole excitons. Therefore, we will refer to circular or linear polariton spin states, excited from circularly or linearly polarized resonant photons, using the literature definitions of circular and linear exciton spin states [16].

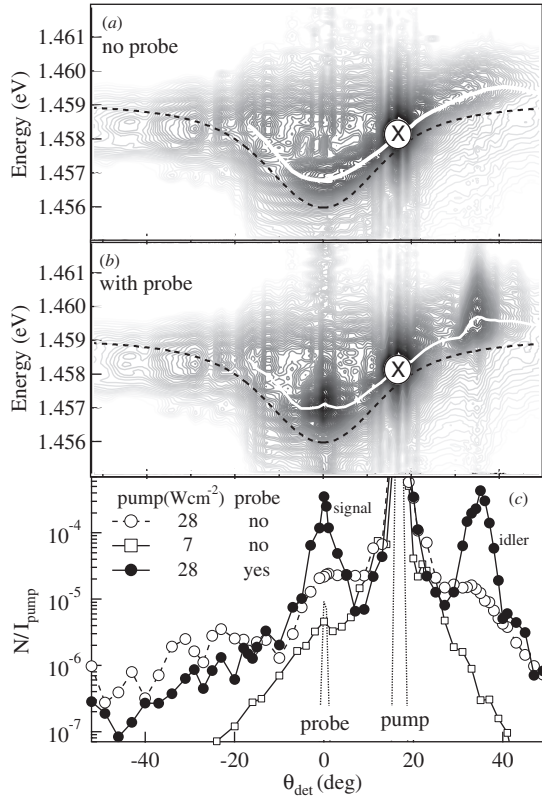


Figure 3. Contour maps of the time-integrated PL spectra versus angle for a 28 W cm^{-2} pump pulse at 16.5° (\times). The white line marks the energy position of the peak PL, while the dotted line is the lower polariton dispersion. (a) Spontaneous and self-stimulated PL emission. (b) Probe-stimulated PL emission showing the signal gain at 0° and idler beam at 35° . (c) Normalized lower branch polariton emission versus angle with (\bullet) and without probe (\square , \circ) for pump powers 7 and 28 W cm^{-2} . Angular widths of pump and probe beams are also plotted.

In the stimulated polariton scattering configuration, a pump pulse resonantly injects a reservoir of polaritons at the point of inflection on the lower polariton (LP) branch and a weak probe pulse is sent at normal incidence onto the sample resonant to the LP branch, seeding polaritons of zero in-plane wavevector as shown in figure 1(c). Throughout these experiments the polarization of the probe pulse is kept right circular whereas we change the pump polarization from right to left circular. Hence this linearly varies the relative circular spin populations (labelled $|\pm 1\rangle$) of the pump-injected polaritons while keeping the pump intensity constant [17].

In what follows, we characterize the pumping light by its circular polarization degree, $\rho = \frac{I^+ - I^-}{I^+ + I^-}$, where I^+ is the intensity of the right-circular component of the pump pulse and I^- is the intensity of its left-circular component. The experimental values of the polarization components for the emitted signal versus ρ are presented in figures 4(a)–(c), as was demonstrated in [17].

From figure 4, the spin selection rules of the stimulated polariton scattering are evident for co- and cross-circular pump–probe polarization ($\rho = \pm 1$). Stimulation occurs only when both pump and probe beams inject polaritons of the same circular spin ($\rho = 1$). We observe that the linear components of the signal unexpectedly exhibit oscillations versus the circular

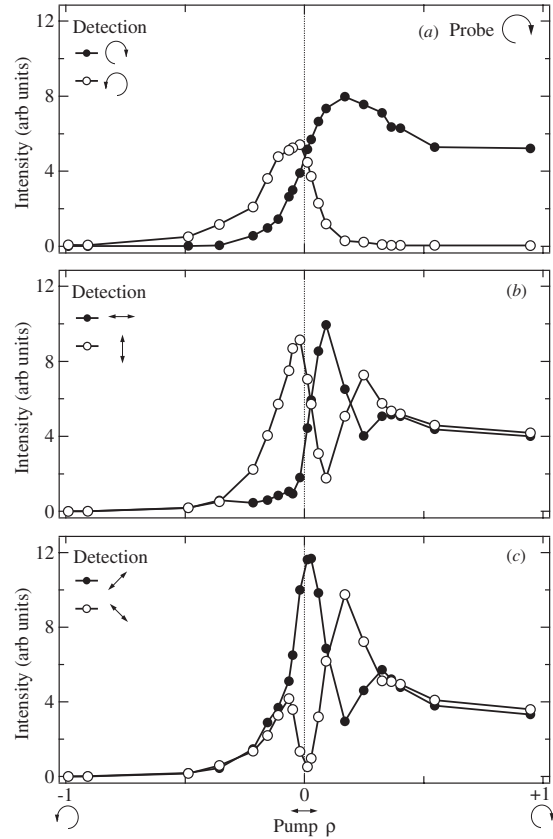


Figure 4. Emitted signal intensities decomposed into (a) circular, (b) linear and (c) linear diagonal polarizations as a function of the circularity of the pump. The probe is right-circular polarized.

polarization degree of pump. Furthermore, we observe that for *horizontal* linear pump polarization ($\rho = 0$) the signal emission is *diagonally* linearly polarized. This feature cannot be derived from stimulation of polariton scattering, since we seed only polaritons of one circular spin state ($|+1\rangle$), whereas diagonally linearly polarized signal emission comes from linear polariton states (a superposition of both circular spin states). To proceed, we must assume that linear polariton spin states can stimulate the scattering of any linear polariton spin state, independent of the constituent linear exciton spin alignment. Therefore, the diagonal linear polarization of the emitted signal indicates that pump-injected polaritons with horizontal linear spin ($|H\rangle$) must have been stimulated by polaritons with diagonal linear spin ($|H'\rangle$) [16].

To reveal the mechanism that leads to occupation of this non-seeded diagonal linear spin state we make use of the Poincaré sphere that is a 3D polarization space in which any polarization state can be expressed as a vector on the orthogonal basis of the three polarization degrees, figure 5(a). For each polarization depicted in figure 5 we have noted the corresponding excited polariton spin state.

For horizontal linear pump polarization ($\rho = 0$), the initial probe-injected polaritons of circular spin lead to the creation of polaritons of diagonal linear spin ($|H'\rangle$) (to give rise to the observed diagonal linear polarization of the emitted signal) by precessing around the pump polarization vector (or $|H\rangle$ polariton spin), as seen in figure 5(a). As a check, we have confirmed that for vertical linear pump polarization

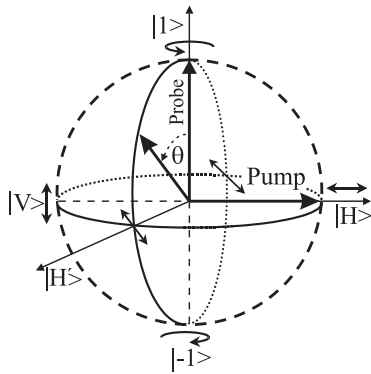


Figure 5. Rotation of the circular polariton spin, S_c , of the probe pulse around the effective magnetic field created by the much stronger pump pulse of linear polariton spin, $|H\rangle$, that results on a probe projection on the diagonal linear polariton spin state.

($\rho = 0$), the initial circular probe gives rise to signal emission of the opposite diagonal linear polarization. This observation suggests that polaritons of circular spin undergo Larmor precession around a pump-induced effective magnetic field.

The origin of this effective magnetic field is the alignment of the constituent exciton dipole moments parallel to the external electric field plane, which in the case of linear pump polarization creates an energy splitting between the TE and TM modes in the quantum well plane due to the Coulomb dipole–dipole interaction and long-range exchange exciton–exciton interaction [18]. This energy splitting creates an effective magnetic field along the pump polarization vector which exercises a torque on exciton spin states perpendicular to the magnetic field direction. The probe spin precession angle takes values in the range of $\theta \in (0, \pi/2]$, within the pump pulse duration, since signal emission comes from only one diagonal linear polariton spin state. This splitting is estimated to be of the order of a few 10 s of μeV , which is smaller than the spectral resolution of the monochromator used in this study. This optically induced energy splitting of the exciton resonance in two orthogonal linear polarizations has been invoked to explain experimental results [19, 20], however, has never been justified theoretically in detail nor observed experimentally to the best of our knowledge.

In the CW regime the signal and idler emission is unpolarized for a linearly polarized pump. In this case, since there is no probe, there is no seed from any linear exciton spin state. The emitted signal and idler originate from the spontaneous pair scattering of polaritons [21], which over a long time yields equal populations in all linear polariton spin states (which lie on the equator of figure 5(a)) and therefore all possible linear emission polarizations, which results in unpolarized signal emission. For a circularly polarized pump, the spontaneous pair scattering of polaritons yields signal and idler of the same circular polarization, since we create polaritons of only one circular spin state.

In table 1 we have summarized the polarization dependence of the signal and idler for the basic pump polarizations (horizontal and co-/cross-circular to the probe) both in the pulsed and CW regimes (no probe). It is also worth mentioning that the spin dynamics under non-resonant pulsed excitation were recently investigated in a CdTe QW semiconductor microcavity by Martin *et al* [22].

Table 1. Polarization of the emitted signal and idler in the pulsed and CW regimes for the elementary pump polarizations.

Pump	Probe	Signal	Idler
Pulsed regime			
σ^+	σ^+	σ^+	σ^+
σ^-	σ^+	No signal	No idler
\leftrightarrow	σ^+	\swarrow	\downarrow
\downarrow	σ^+	\searrow	\leftrightarrow
CW regime			
σ^+	σ^+	σ^+	σ^+
σ^-	σ^-	σ^-	σ^-
\leftrightarrow		Non-polarized	Non-polarized
\downarrow		Non-polarized	Non-polarized

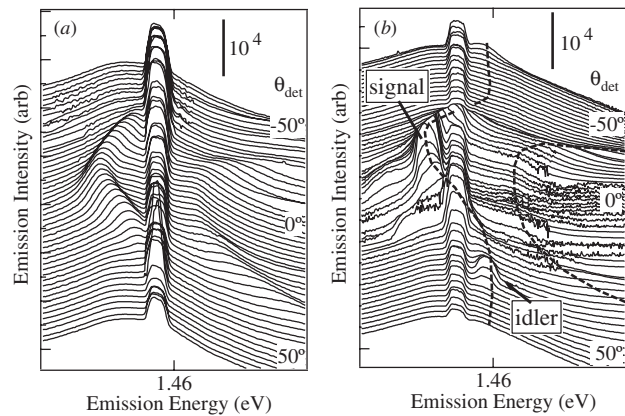


Figure 6. Photoluminescence spectra taken at angles between -50° and $+50^\circ$ when excited at (a) 27.6° and (b) 16.5° with CW pump beam tuned to the lower polariton branch. Polariton dispersion is clearly resolved in both cases. μOPO regime is observed when pumping at 16.5° with signal and idler beams clearly showing at 0° and 35° , respectively.

5. Parametric oscillation

Polariton dynamics in the steady state regime under continuous wave excitation offers new possibilities for manipulating emission from microcavities. CW polariton dynamics is very different compared to the pulsed excitation regime due to the much lower peak powers resulting in a completely different distribution of polaritons along the dispersion. In our experiments we demonstrated the first optical parametric oscillation of a microcavity or (μOPO) [23]. When pumped by a CW near-infrared laser at the critical angle (identified in time-resolved measurements), the device coherently radiates signal and idler beams of different wavelengths in different directions. The signal emission from a microcavity in this regime has small angular divergence, is coherent and monochromatic, strongly resembling laser emission. The line width of the emission has been interferometrically measured [24] and is found to be below 500 MHz, indicating a collective phase coherence time >1 ns, three orders of magnitude longer than that of the excitons at this density. The process responsible is identical to that described in the pulsed experiments (i.e. scattering of two pump polaritons into the signal and idler modes). Figure 6(b) shows that parametric scattering dominates emission from a semiconductor microcavity when pumped at the magic angle

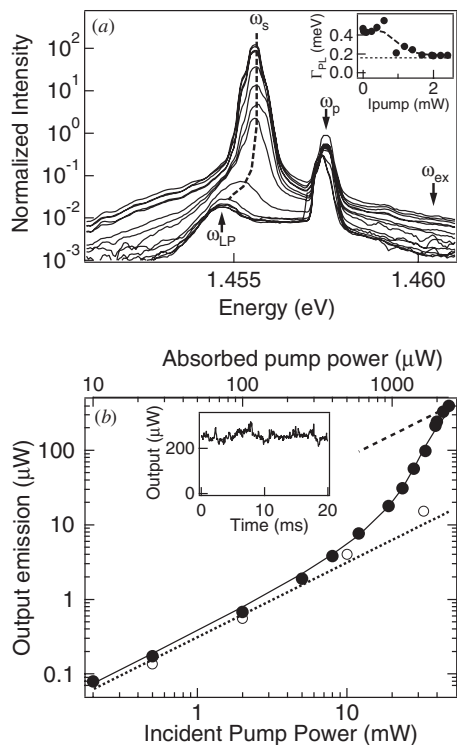


Figure 7. (a) Power-dependent emission spectra of the signal beam at 0° normalized to the pump power (incident at 16.5°). At high and low powers the emission is linear, while nonlinear at intermediate powers. The energies of lower polariton (ω_{LP}), pump (ω_p), signal (ω_s) and bare exciton (ω_{ex}) are marked. Inset: FWHM emission line width versus absorbed pump power. Polariton splitting in this sample is $\hbar\Omega = 7$ meV and the data are taken at zero detuning. (b) Extracted integrated power output versus incident and absorbed powers for excitation at 16.5° at energies on the lower polariton (solid) and upper polariton (open). The line is a fit described in the text. Inset: signal beam output.

(here 16.5°). In complete contrast, when the microcavity is excited at 27.6° no pair scattering is observed due to its suppression by the dispersion relation and instead emission into a broad cone of $\pm 20^\circ$ is observed resolving the polariton dispersion.

The resulting OPO device is the smallest reported because the gain in this device is based on a stimulated scattering mechanism and is exponentially dependent on the pump power. It can be as high as 10^6 cm^{-1} [25], and is larger than that of any other nonlinear material [26, 27]. This very efficient gain mechanism mainly arises from the resonant field enhancement in the cavity of pump, signal and idler, and is responsible for our successfully shrinking such devices by a factor of 10 000.

The emission of the signal beam shows a dramatic superlinear increase (with simultaneous decrease in the line width) when increasing pump power (figure 7(a)). The spectrally integrated output power of this device is linear at low pump powers with an apparent threshold at moderate pump powers around 40 mW and increases linearly after the threshold (figure 7(b)). The power dependence of a laser reveals important information about the laser operation. One of the crucial parameters in the laser design is the number of modes into which the gain medium can spontaneously radiate. A fit to the power dependence which takes into account the

number of modes into which the laser can spontaneously decay [23] suggests that the number of available spontaneous modes is ~ 40 . Restriction of these modes in VCSELs by lateral confinement reduces the lasing threshold and improves the device operation. Strikingly μ OPOs do not require lateral confinement because the polariton dispersion provides a trap for polaritons in momentum space removing the possibility of emission into many in-plane photon modes. The inset of figure 7(b) shows that when the absorbed pump power is 1.25 mW the signal output is $250 \mu\text{W}$ with a maximum conversion efficiency of 20%.

6. Ring emission

Although many experiments on nonresonant excitation have demonstrated nonlinear emission from the bottom of the trap which was attributed to final state stimulation, they have failed to definitively explain the mechanism by which polaritons lose their energy and end up at the bottom of the trap with phonons [5, 28], disorder [14, 29], and exciton–exciton scattering processes all suggested in [7, 30, 31]. A bottleneck in the exciton relaxation is formed at the neck of the trap due to the dramatically reduced density of states. Particularly, Huang *et al* have proposed a scattering process in which two polaritons from the reservoir are scattered into the lower and upper polariton states both at $k_{\parallel} = 0$. Our recent experiments indeed showed that Coulomb-mediated exciton–exciton scatterings dominate the exciton relaxation from the reservoir [32]. In these experiments we utilized resonant injection of a cold exciton gas into the bottleneck region and observed strong emission in the form of the ring with its energy lying on the lower polariton branch just below the exciton energy. With increasing exciton density the radius of the ring shrinks until it collapses into a spot at the bottom of the trap. The emission energy follows the polariton dispersion although it is not clear whether the strong coupling is intact throughout this process. At large negative detunings used in these experiments the lower polariton branch is indistinguishable from the cavity mode branch in the region of the trap making the judgement about strong coupling difficult.

Such ring emission should not be confused with other similar observations in which annular emission peaked at the excitation angle was seen resulting from resonant Rayleigh scattering of polaritons due to disorder [33–35].

A recently developed theory confirms these observations and reproduces the density and temperature dependence of the ring emission [36]. According to this model, exciton–polariton scattering is clearly the dominating mechanism for the relaxation into the trap (figure 8). In this process two excitons from a thermalized reservoir scatter with one of them ending up inside the trap and the other scattered to higher energy on the lower polariton branch. It should be noted that a quadratic dispersion relation cannot support such exciton pair scattering and it is only possible due to dispersion engineering in microcavities. Such scattering is shown to produce a polariton population with an occupancy that has a maximum at a given energy below the exciton energy [36]. Since the emission is directly related to the polariton population, it has a ring shape in agreement with the experiment, while the energy loss is linearly dependent on the exciton density

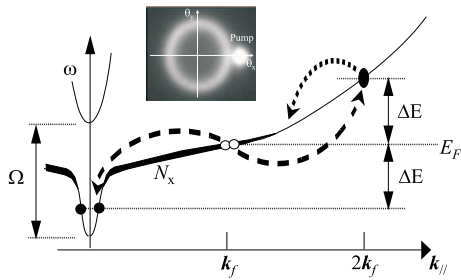


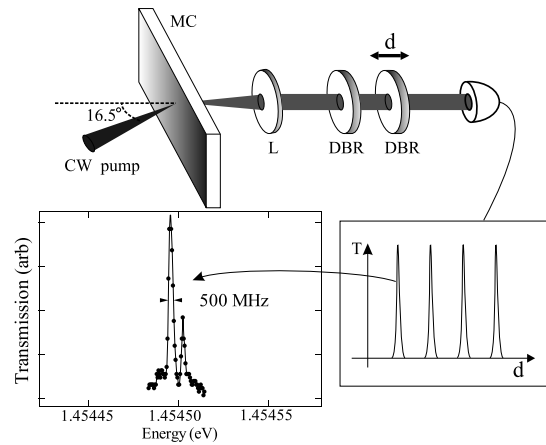
Figure 8. Far-field image of the annular output emission for negative detuning $\Delta = -15$ meV when pumped at $\theta_p = 30^\circ$ and a temperature $T = 10$ K. The dominating relaxation process is the exciton pair scattering with a maximum energy exchange, ΔE .

and the temperature. This scattering mechanism can be useful for creating a Bose–Einstein condensate (BEC) at the bottom of the trap provided that strong coupling is intact. This requires the use of alternative materials such as CdTe microcavities since these structures can withstand much higher excitation densities due to the smaller exciton radius [37]. Above a critical pump density macroscopic occupancies can be achieved in the ground state of the trap. An alternative approach in semiconductor microcavities for achieving BEC has been also proposed by us which relies on an efficient electron–polariton scattering mechanism in n-doped microcavities [38–41]. It remains to be seen whether it is indeed possible to create a polariton laser or BEC of polaritons from an incoherent thermalized reservoir. This kind of laser has one particular characteristic in that it works without population inversion and relies on efficient pair scattering and fast thermalization of the carrier reservoir. Quantum cascade lasers and Bloch oscillators are few examples of inversionless lasers attracting much recent interest.

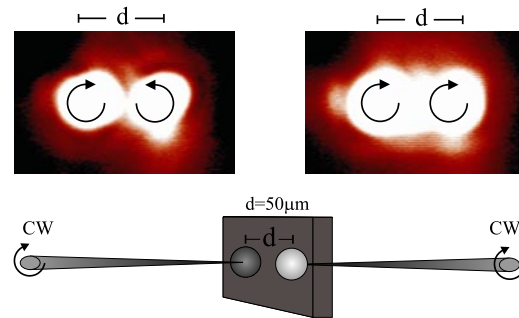
7. Polariton condensates

There has been continued interest in the possibility that excitons in semiconductors can condense into a macroscopic phase-coherent state in analogy with Bose–Einstein atomic condensates. Atomic condensates and superconducting junctions are already being used in precision measurements of local gravitational and magnetic fields [42]. Although excitons are bosons, direct evidence of their condensation has yet to be seen although recent work is tantalizing [43]. On the other hand, polaritons are particularly favourable for demonstration of such effects due to their small effective mass requiring lower particle densities and resulting in higher critical temperatures for this phase transition. Since the lifetime of polaritons is short compared to their thermalization time, the recent experimental attempts have mainly focused on non-equilibrium phase transitions [21].

The results of parametric oscillation have another intriguing aspect. That is, that the spectral narrowing of the signal emission observed in the regime of parametric oscillation shows that like a laser, the system possesses macroscopic coherence (figure 9(a)) [24]. The interferometric resolution of the signal emission, reveals a coherence lifetime well beyond the polariton lifetime (~ 5 ps) of the pump laser suggesting that the system undergoes a true phase transition to form a single, macroscopically occupied state



(a)



(b)

Figure 9. (a) Measured polariton emission spectrum using a plane Fabry–Perot interferometer of spectral resolution $4 \mu\text{eV}$. (b) Near-field images of two polariton reservoirs, with $50 \mu\text{m}$ separation, pumped by cross- and co-circularly polarized CW beams (left and right images, respectively).

[21] that is quantum mechanically coherent (figure 9(a)). Support for this description is provided by the clear observation of stimulated scattering of other polaritons into the macroscopically occupied mode, a characteristic property of bosons.

Therefore, polaritons do exhibit bosonic behaviour, however, strictly speaking they cannot condense as they are 2D particles. They are subject to a Kosterlitz–Thouless phase transition towards a superfluid phase and to local quasi-condensation [44]. This state can be called a polariton condensate since it has number of similarities with the BEC but is different in that it is a non-equilibrium 2D superfluid. Polaritons having a very short lifetime leak out of the trap and a continuous injection of new polaritons is required to maintain the condensate. Phase coherence is provided due to the fact that polaritons which are already in the trap are well protected from scattering with other polaritons and excitons in the system. Very recently, a coherence prolongation was observed as the non-resonant pumping intensity was increased [45]. This observation still needs to be confirmed. In a polariton condensate, the macroscopic coherence of the state extends throughout the structure via the exciton component, which implies spatially dependent condensate interactions. In addition, spin-dependent interactions are possible as we can selectively excite condensates of a particular spin. Figure 9(b) shows the near-field images of two adjacent ($50 \mu\text{m}$) polariton reservoirs resonantly injected at the ground polariton state in

the case of co- and cross-circular CW beams. It is evident that in the case of co-circular polarized beams the two polariton reservoirs spatially interact with each other. The dynamics of this spatially separated polariton condensates have not yet been understood.

Understanding the polariton dynamics on the newly engineered dispersion relations together with the exploitation of polariton Bose-condensation effects will offer new possibilities for making ultra-sensitive interferometric devices as well as low threshold light emitters. The use of large band-gap semiconductors GaN, ZnO or of organic materials should allow the operation of such devices at room temperatures.

8. Conclusions

In this paper, we have reviewed the resonant stimulated scattering of polaritons. We have shown the very different emission properties of polaritons in k -space when in the strong coupling regime. We introduced a phenomenological approach that explains the spin dynamics of the stimulated scattering of polaritons. The operation of microcavities as optical parametric oscillators and ring emitters has been described. Finally, based on bosonic properties of polaritons, such as the stimulated scattering by final state occupation and recent observations of increasing optical coherence in polariton ground state emission with non-resonant pumping intensity, we have discussed the possibilities of a polariton condensate.

Acknowledgments

We gratefully acknowledge the contribution of Professor J J Baumberg as principal investigator of this research. We have also greatly benefited from the interactions with M S Skolnick, D M Whittaker, C Ciuti, G Malpuech and A V Kavokin. This work has been supported by the EU RTN 'CLERMONT' programme, contract no HPRN-CT-1999-00132 and HPMT-CT-1999-00191, EPSRC GR/M43890 and HEFCE JR98SOBA.

References

- [1] Weisbuch C, Nishioka M, Ishikawa A and Arakawa Y 1992 *Phys. Rev. Lett.* **69** 3314
- [2] Yamamoto Y 2000 *Nature* **405** 629–30
- [3] Keldysh L V 1995 *Bose–Einstein Condensation* ed A Griffin, D W Snoke and S Stringari (Cambridge: Cambridge University Press) p 246
- [4] Imamoglu A, Ram R J, Pau S and Yamamoto Y 1996 *Phys. Rev. A* **53** 4250
- [5] Senellart P and Bloch J 1999 *Phys. Rev. Lett.* **82** 1233
- [6] Dang L S, Heger D, André R, Boeuf F and Romestain R 1998 *Phys. Rev. Lett.* **81** 3920
- [7] Tartakovskii A I, Emam-Ismaïl M, Stevenson R M, Skolnick M S, Astratov V N, Whittaker D M, Baumberg J J and Roberts J S 2000 *Phys. Rev. B* **62** R2283
- [8] Snoke D 2002 *Science* **298** 1368
- [9] Kisilev A V *et al* 1975 *Phys. Status Solidi b* **72** 161
- [10] Wicksted J, Matsushita M, Cummins H Z, Shigenari T and Lu X Z 1984 *Phys. Rev. B* **29** 3350
- [11] Savvidis P G, Baumberg J J, Stevenson R M, Skolnick M S, Whittaker D M and Roberts J S 2000 *Phys. Rev. Lett.* **84** 1547
- [12] Savvidis P G, Baumberg J J, Stevenson R M, Skolnick M S, Whittaker D M and Roberts J S 2000 *Phys. Rev. B* **62** R13278
- [13] Kira M, Jahnke F, Koch S W, Berger J D, Wick D V, Nelson T R Jr, Khitrova G and Gibbs H M 1997 *Phys. Rev. Lett.* **79** 5170
- [14] Fan X, Wang H, Hou H Q and Hammons B E 1997 *Phys. Rev. B* **56** 15256
- [15] Ciuti C, Schwendimann P and Quattropani A 2000 *Phys. Rev. B* **62** R4825
- [16] Ivchenko E L and Pikus G E 1995 *Superlattices and Other Heterostructures. Symmetry and Optical Phenomena* (Berlin: Springer)
- [17] Lagoudakis P G, Savvidis P G, Baumberg J J, Whittaker D M, Eastham P R, Skolnick M S and Roberts J S 2002 *Phys. Rev. B* **65** 161310 (R)
- [18] Andreani L C and Bassani F 1990 *Phys. Rev. B* **41** 7536
- [19] Oudar J L, Migus A, Hulin D, Grillon G, Etchepare J and Antonetti A 1984 *Phys. Rev. Lett.* **53** 384
- [20] Kavokin A, Lagoudakis P G, Malpuech G and Baumberg J J 2003 *Phys. Rev. B* **67** 195321
- [21] Stevenson R M, Astratov V N, Skolnick M S, Whittaker D M, Emam-Ismaïl M, Tartakovskii A I, Savvidis P G, Baumberg J J and Roberts J S 2000 *Phys. Rev. Lett.* **85** 3680
- [22] Martin M D, Aichmayr G, Viña L and André R 2002 *Phys. Rev. Lett.* **89** 077402
- [23] Baumberg J J, Savvidis P G, Stevenson R M, Tartakovskii A I, Skolnick M S, Whittaker D M and Roberts J S 2000 *Phys. Rev. B* **62** R16247
- [24] Baumberg J, Savvidis P G, Lagoudakis P G, Martin M D, Whittaker D M, Skolnick M S and Roberts J S 2002 *Physica E* **13** 385
- [25] Baumberg J J 2002 *Phys. World* **15** 37
- [26] Dunn M H and Ebrahimzadeh M 1999 *Science* **286** 1513
- [27] Myers L E, Eckardt R C, Fejer M M, Byer R L, Bosenberg W R and Pierce J W 1995 *J. Opt. Soc. Am. B* **12** 2102
- [28] Boeuf F, André R, Romestain R, Dang L S, Pronne E, Lampin J F, Hulin D and Alexandrou A 2000 *Phys. Rev. B* **62** R2279
- [29] Müller M, Bleuse J and Andre R 2000 *Phys. Rev. B* **62** 16886
- [30] Senellart P, Bloch J, Sermage B and Marzin J Y 2000 *Phys. Rev. B* **62** R16263
- [31] Huang R, Yamamoto Y, André R, Bleuse J, Muller M and Ulmer-Tuffigo H 2000 *Phys. Rev. B* **65** 165314
- [32] Savvidis P G, Baumberg J J, Porras D, Whittaker D M, Skolnick M S and Roberts J S 2002 *Phys. Rev. B* **65** 073309
- [33] Freixanet T, Sermage B, Bloch J, Marzin J Y and Planel R 2000 *Phys. Rev. B* **60** R8509
- [34] Houdré R, Weisbuch C, Stanley R P, Oesterle U and Ilegems M 2000 *Phys. Rev. B* **61** R13333
- [35] Houdré R, Weisbuch C, Stanley R P, Oesterle U and Ilegems M 2000 *Phys. Rev. Lett.* **85** 2793
- [36] Porras D, Ciuti C, Baumberg J J and Tejedor C 2002 *Phys. Rev. B* **66** 085304
- [37] Saba M *et al* 2002 *Nature* **414** 731
- [38] Qarry A, Ramon G, Rapaport R, Cohen E, Ron A, Mann A, Linder E and Pfeiffer L N 2003 *Phys. Rev. B* **67** 115320
- [39] Malpuech G, Kavokin A, Di Carlo A and Baumberg J J 2002 *Phys. Rev. B* **65** 153310
- [40] Malpuech G, Di Carlo A, Kavokin A, Baumberg J J, Zamfirescu M and Lugli P 2002 *Appl. Phys. Lett.* **81** 412
- [41] Lagoudakis P G, Martin M. D, Baumberg J J, Qarry A, Cohen E and Pfeiffer L N 2003 *Phys. Rev. Lett.* **90** 206401
- [42] Dalfovo F, Giorgini S, Pitaevskii L P and Stringari S 1999 *Rev. Mod. Phys.* **71** 463
- [43] Butov L V, Gossard A C and Chemla D S 2002 *Nature* **418** 751
- [44] Kavokin A, Malpuech G and Laussy F P 2003 *Phys. Lett. A* **306** 187
- [45] Deng H, Weihs G, Santori C, Bloch J and Yamamoto Y 2002 *Science* **298** 199